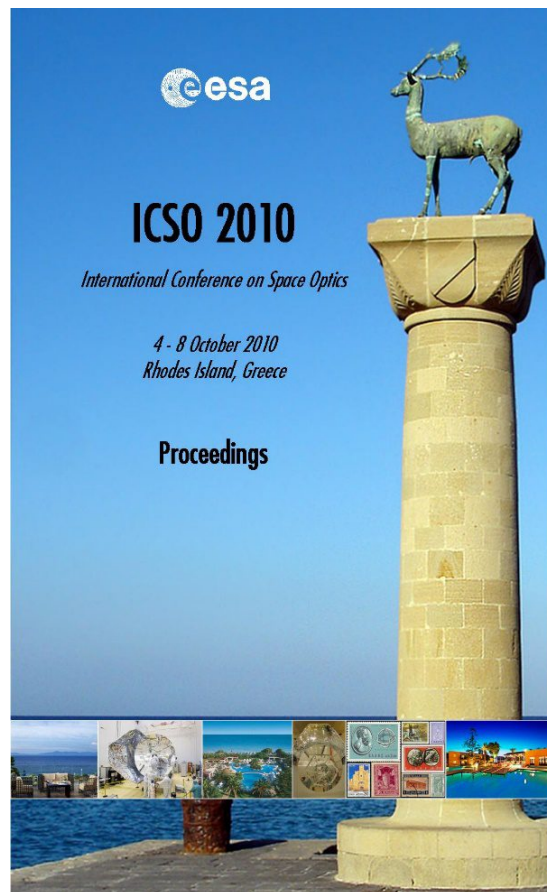


International Conference on Space Optics—ICSO 2010

Rhodes Island, Greece

4–8 October 2010

*Edited by Errico Armandillo, Bruno Cugny,
and Nikos Karafolas*



Multi-mode optical fibers for connecting space-based spectrometers

W. T. Roberts, C. A. Lindenmish, S. Bender, E. A. Miller, et al.



International Conference on Space Optics — ICSO 2010, edited by Errico Armandillo, Bruno Cugny, Nikos Karafolas, Proc. of SPIE Vol. 10565, 105651A · © 2010 ESA and CNES
CCC code: 0277-786X/17/\$18 · doi: 10.1117/12.2309137

MULTI-MODE OPTICAL FIBERS FOR CONNECTING SPACE-BASED SPECTROMETERS

W. T. Roberts¹, C. A. Lindenmish¹, S. Bender², E. A. Miller¹, E. Motts¹, M. Ott³, F. LaRocca³, J. Thomes³

¹*Jet Propulsion Laboratory, 4800 Oak Grove Drive, Pasadena, CA, 91208, USA*

²*Los Alamos National Laboratory, PO Box 1663, Los Alamos, NM, 87545, USA*

³*Goddard Space Flight Center, Mail Code 130, Greenbelt MD, 20771, USA*

I. INTRODUCTION

Laser spectral analysis systems are increasingly being considered for *in situ* analysis of the atomic and molecular composition of selected rock and soil samples on other planets [1][2][3]. Both Laser Induced Breakdown Spectroscopy (LIBS) and Raman spectroscopy are used to identify the constituents of soil and rock samples *in situ*. LIBS instruments use a high peak-power laser to ablate a minute area of the surface of a sample. The resulting plasma is observed with an optical head, which collects the emitted light for analysis by one or more spectrometers. By identifying the ion emission lines observed in the plasma, the constituent elements and their abundance can be deduced. In Raman spectroscopy, laser photons incident on the sample surface are scattered and experience a Raman shift, exchanging small amounts of energy with the molecules scattering the light. By observing the spectrum of the scattered light, it is possible to determine the molecular composition of the sample.

For both types of instruments, there are advantages to physically separating the light collecting optics from the spectroscopy optics. The light collection system will often have articulating or rotating elements to facilitate the interrogation of multiple samples with minimum expenditure of energy and motion. As such, the optical head is often placed on a boom or an appendage allowing it to be pointed in different directions or easily positioned in different locations. By contrast, the spectrometry portion of the instrument is often well-served by placing it in a more static location. The detectors often operate more consistently in a thermally-controlled environment. Placing them deep within the spacecraft structure also provides some shielding from ionizing radiation, extending the instrument's useful life. Finally, the spectrometry portion of the instrument often contains significant mass, such that keeping it off of the moving portion of the platform, allowing that portion to be significantly smaller, less massive and less robust.

Large core multi-mode optical fibers are often used to accommodate the optical connection of the two separated portions of such instrumentation. In some cases, significant throughput efficiency improvement can be realized by judiciously orienting the strands of multi-fiber cable, close-bunching them to accommodate a tight focus of the optical system on the optical side of the connection, and splaying them out linearly along a spectrometer slit on the other end.

For such instrumentation to work effectively in identifying elements and molecules, and especially to produce accurate quantitative results, the spectral throughput of the optical fiber connection must be consistent over varying temperatures, over the range of motion of the optical head (and its implied optical cable stresses), and over angle-aperture invariant of the total system. While the first two of these conditions have been demonstrated[4], spectral observations of the latter present a cause for concern, and may have an impact on future design of fiber-connected LIBS and Raman spectroscopy instruments. In short, we have observed that the shape of the spectral efficiency curve of a large multi-mode core optical fiber changes as a function of input angle.

II. EXPERIMENT

A. Apparatus

To investigate the aforementioned effect, we assembled the test apparatus shown in Fig 1. A fiber-coupled deuterium-halogen source is collimated by a fixed-lens attached to a micrometer-driven translation stage. Initial observations of the output of this fiber showed various angles with non-uniform intensities and spectral effects, so the delivery fiber was intentionally kinked to assure mode randomization throughout the fiber. The collimated light is directed toward the circular end of the fiber bundle under test. The distance from the center of the post mounting the collimating system to the fiber bundle face is approximately 84 mm.

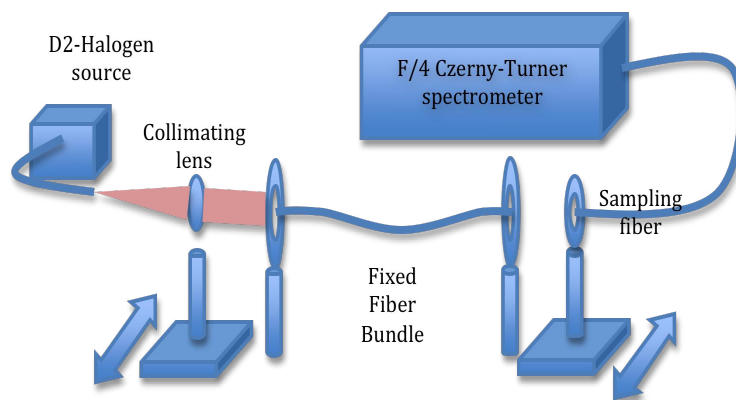


Fig. 1 Experimental setup for investigating spectro-angular fiber throughput

A bare multi-mode fiber on a micrometer-driven translation stage is used to sample the bundle output at various angles with respect to the bundle face. The distance from the output (line) face of the fiber bundle to the rotation axis of the sampling-fiber post is approximately 30 mm. The sampled light from the fiber bundle is fed into an F/4 Czerny-Turner spectrometer with automated filter wheel gain-setting systems.

To obtain a baseline for comparison, the collimating lens was set to direct light down the axis of the fiber bundle. The sampling fiber was set up in a similar fashion to maximize the throughput. This measurement became the baseline measurement $b(\lambda)$ to which other measurements at other angles $m(\lambda)$ were compared. The light source was also blocked with an internal shutter to obtain a background measurement $d(\lambda)$, mainly correcting for the varying dark counts observed when the spectrometer gain was changed over different wavelength regions. At each wavelength, the relative throughput was computed according to

$$r(\lambda) = \frac{m(\lambda) - d(\lambda)}{b(\lambda) - d(\lambda)}. \quad (1)$$

Note that this assumes that the background level is constant, and the throughput is calculated relative to the on-axis input measurement. The detector sensitivity drops rapidly at longer wavelengths, such that the dark noise $d(\lambda)$ is a much larger fraction of the detected signal at these wavelengths. Hence, the throughput curves show significantly more noise at longer wavelengths, and individual narrow features in the data should not be considered significant. Instead, we look for the trend in the data.

B. Test Article

The test article consisted of a short bundle of 19 fibers, used to connect a spectrally selective optical ‘demultiplexer’ to one of three grating spectrometers. Each of the 19 fibers in the bundle was a multimode 0.12 NA fiber, with a 50 μm diameter high-index core and a 55 μm lower-index cladding. The fibers were stripped of their buffer and jacket material on each end, and packed in a single bored-out FC ferrule. On the input end of the bundle where the image of the fiber-conducted plasma light is expected to be circularly symmetrical with a diameter of approximately 250 μm , the fibers are closely packed together in an arrangement with one fiber in the center, a ring of 6 fibers immediately surrounding the central fiber, and an outer ring of 12 fibers surrounding that.

At the other end of the bundle, the fiber tips are splayed out linearly to improve coupling to the spectrometer slit. The arrangement of these fiber tips comprises a pseudo-slit with a length of slightly over 1 mm, and an effective slit-width of approximately 50 μm . It was also packaged in an FC connector ferrule. The pseudo-slit arrangement does not have any appreciable effect on the output angles of light, such that the light pattern projected directly out of the pseudo-slit appears circular just a centimeter away from the fiber ends. The manufacturer was instructed to place the central fiber from the circular end in the center of the pseudo-slit, the inner ring of 6 fibers on the circular end immediately surrounding the central fiber of the pseudo-slit, and the remaining fibers at the outer portion of the pseudo-slit, though compliance with this has not been confirmed by measurement.

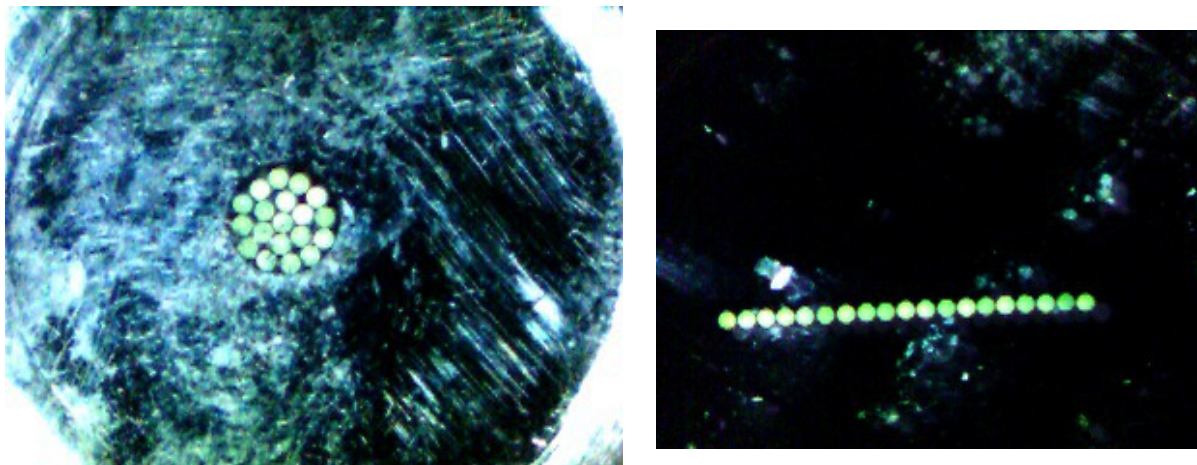


Fig. 2 Images of the fiber bundle ends showing the close-pack bundle on the input end (left) and pseudo-slit on the output end (right).

The bundle of jacketed fibers between the two connector ends was jacketed with a shrink tubing to reduce the chance of snagging and damaging the individual fiber strands. The entire length of the bundle from end-to-end was 150 mm. It was built with a resting arc of roughly 50 degrees to partially accommodate a necessary bend of 110 degrees from the optical demultiplexer to the spectrometer input. Images of the bundle ends on both the close-bunched input end and the pseudo-slit output end are shown in Figure 2.

C. Measurements

Spectral measurements were first obtained with the collimated beam transmitting directly down the central axis of the fiber bundle. The sampling fiber at the output end was moved to different locations to sample the spectral output at different numerical aperture (NA) values ranging from -0.03 to 0.10. In these data, shown in Fig. 3 below, a few significant features stand out. First, the angular output distribution is roughly consistent with a Gaussian output with an NA of 0.1. It is approximately symmetrical about the axis (as shown by the similarity of the 0.03 NA and -0.03 NA curves). The average values at each measured location correspond roughly to the amount of light in a Gaussian at the indicated angle. Apparently, light is scattered to higher-order modes in the optical fibers of the bundle, but the output is not scattered evenly among the guiding modes.

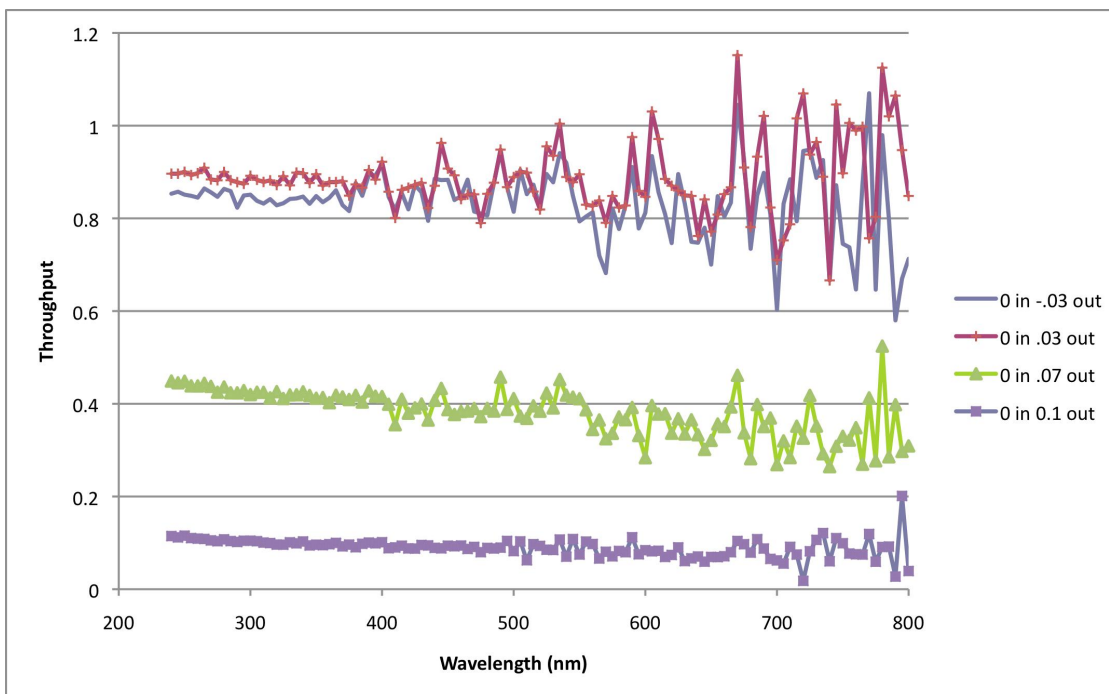


Fig. 3 Spectro-spatial measurements showing a roughly Gaussian drop-off in intensity as a function of output angle, with little spectral variation. All plots generated with input light along fiber axis.

The second observation is that, in this case in which light is launched on-axis, the attenuation is not strongly dependent on wavelength, at least in the 240-800 nm region of the test. Even though the total light intensity was lower at higher NA values, there was little color effect introduced.

After establishing the baseline for light injected down the fiber axis, the input system (located on the first translation stage shown in Fig 1.) was moved so that light was injected from an angle corresponding to 0.05 NA. After translating the input system, the lens collimator was aimed to maximize the amount of light into the fiber once again.

With light entering the fiber at a relatively high angle of 0.05 NA, the character of the output light changed significantly, both in angle-dependant intensity as well as spectral profile, as shown in Fig. 4. All NA values out to NA=0.07 showed almost exactly the same profile, so the output of the fiber in the far-field appears to be a uniform disk with no significant intensity or angular color variation. Extending beyond this central disk to 0.1 NA, the power drops off in roughly equal absolute amounts across the spectrum.

At least as important, however, is the observation that the light launched at higher NA is guided more efficiently at shorter wavelengths, imparting a significant 'blue' color relative to the original input spectrum. Since the emitted light at the highest NA experiences relatively more attenuation of the longer wavelengths, the output of the fiber bundle observed on a card a few centimeters from the bundle tip clearly shows a bluer ring surrounding the uniform-intensity core beam.

III. DISCUSSION

From a conventional ray-optics point of view, the fiber numerical aperture is determined by the relative refractive indices of the core and cladding materials at the interface. The acceptance angle of the fiber is determined by the internal critical angle (the maximum angle at which light will experience total internal reflection)

$$NA = \sqrt{n_{core}^2 - n_{cladding}^2} \quad (2)$$

Though light may be injected into the fiber at higher angles, the lack of total internal reflection results in small amounts of light being transmitted at each reflection, significantly attenuating the signal over distances of a few millimeters.

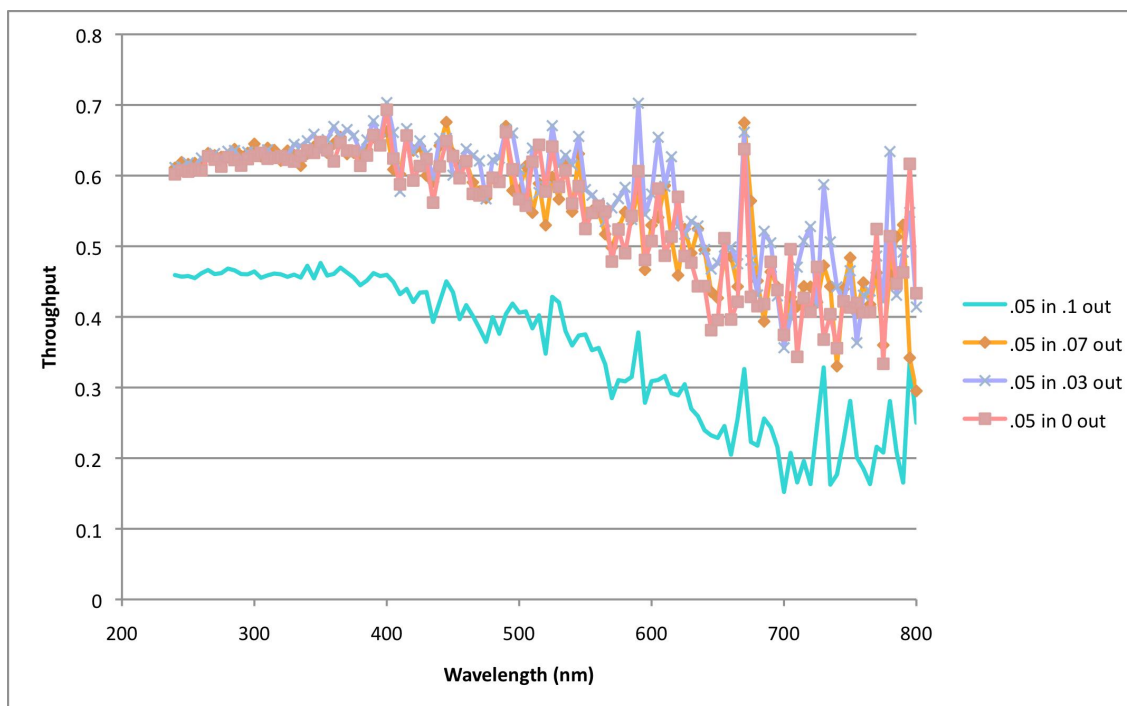


Fig. 4 Spectral measurements at different output angles for an input angle of 0.05 NA.
Proc. of SPIE Vol. 10565 105651A-5

Though fiber manufacturers often refer to a single value for a fiber's numerical aperture, the fact that n_{core} and n_{cladding} vary as a function of wavelength implies that the critical angle (and hence the fiber NA) are spectrally dependent.

Assuming the materials are adequately modeled by the Sellmeier equation [5] and using measured coefficients of an undoped silica core with 1% (by weight) fluorine-doped silica cladding [5]

$$n^2(\lambda) = \sqrt{1 + \sum_{i=1}^3 \frac{A_i \lambda^2}{\lambda^2 - l_i^2}} \quad (3)$$

we interpolate to estimate that a doping level of the silica cladding of 0.77% by weight will give a cutoff NA of 0.11 at 400 μm . However, this simple analysis does not introduce enough spectrally-dependant change to the cutoff wavelength to account for the observed effect, as shown in Fig 5.

This observation has implications for the design of fiber-coupled spectroscopy instruments, particularly instruments attempting to obtain quantitative spectral data. While the fiber coupling can be designed to provide very consistent throughput over thermal swings from -130 C to +70 C, down to 50 mm bend radii, and over large numbers of bend and thermal cycles [4], spectral and angular energy distributions can apparently change as a function of injection angle.

Some instruments make use of a Cassegrain telescope with a large central obscuration to maximize the collected signal for a given optical system mass and volume. However, the central obscuration will result in an angular distribution of light in which light along the central axis is completely missing, and light injected from high off-axis angles (where the angular differential surface area is maximum) dominates. In such cases, the Partial Least Squares (PLS) training sets used to obtain quantitative measurements of elemental and molecular abundances from the spectra must be obtained on comparable systems and under comparable injection angles as the conditions of use.

As an example of a potential concern, an instrument may use a Cassegrain telescope head in which the secondary mirror is moved longitudinally in order to adjust the system focus between samples at near and far ranges. This focusing effect can affect significant changes on the system NA, causing most of the light to be injected at higher angles as the telescope focus changes. Thus, if the PLS training set were generated while the system is at close focus to maximize the training signal, the obtained data can stray more and more from reality as samples at greater and greater ranges are interrogated.

A similar but distinct concern arises in systems that employ pupil stops to limit the amount of light pushed through the system. Again, the system varies the angular distribution of input signal to accommodate pragmatic operational conditions, but may introduce a potential source of error that is particularly difficult to trace.

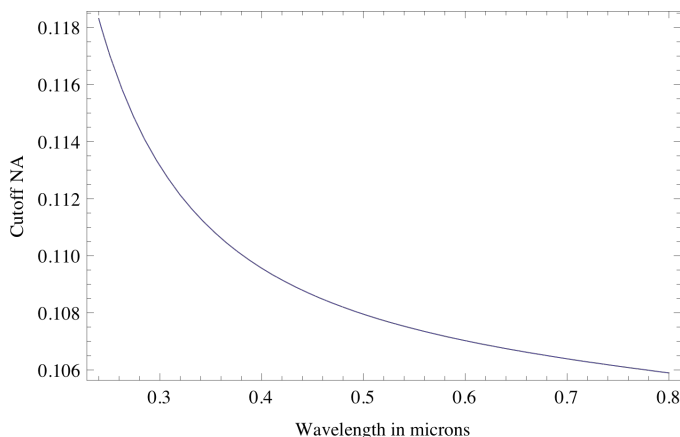


Fig. 5 Calculated fiber angular cutoff NA as a function of wavelength, assuming 0.77% fluorine in the silica cladding layer.

IV. SUMMARY

Designers of space flight instrumentation often have significant incentives to separate the collection optics from the spectral analysis optics in a flight spectrometer, coupling them with a large, multi-mode optical fiber. However, we have observed the tendency of multi-mode optical fibers to affect the spectrum as a function of the numerical aperture of the injected light, resulting in potentially significant sources of calibration error. While we believe this can be adequately calibrated out of the system, it is nevertheless a factor to be considered in the use of multi-mode fiber connections, and attempts to use such fibers in spectral instrumentation.

V. REFERENCES

- [1] N. L. Lanza, R. C. Wiens, S. M. Clegg, A. M. Ollila, S. D. Humphries, H. E. Newsom, and J. E. Barefield, "Calibrating the ChemCam laser-induced breakdown spectroscopy instrument for carbonate minerals on Mars," *Appl. Opt.*, Vol. 49, pp. C211-C217 (2010).
- [2] P. Esposito, *unpublished*, 2009.
- [3] J. L. Lambert, J. Morookian, T. Roberts, J. Polk, S. Smrekar, S. M. Clegg, R. C. Weins, M. D. Dyar, and A. Treiman, Standoff LIBS and Raman Spectroscopy under Venus Conditions, 41st Lunar and Planetary Science Conference (2010), paper 2608, March 2010.
- [4] C. A. Lindensmith, W. T. Roberts, M. Meacham, M. Ott, F. LaRocca, J. Thomes, "Development and Qualification of a Fiber Optic Cable for Martian Environments", unpublished, October 2010.
- [5] J. W. Fleming and D. L. Wood, "Refractive index dispersion and related properties in fluorine doped silica," *Appl. Opt.*, Vol. 22 No. 19, pp. 3102-3104, October 1983.

VI. ACKNOWLEDGEMENTS

The research described in this paper was carried out at the Jet Propulsion Laboratory, California Institute of Technology, under a contract with the National Aeronautics and Space Administration. Copyright 2010. All rights reserved.